

Radiation Effects and Defects in Solids: Incorporating Plasma Science and Plasma Technology

Publication details, including instructions for authors and subscription information:

<http://www.tandfonline.com/loi/grad20>

Modification of polyethylene terephthalate by proton irradiation

N. L. Singh^a, Nilam Shah^a, C. F. Desai^a, K. P. Singh^b & S. K. Arora^c

^a Department of Physics, M. S. University of Baroda, Vadodara, 390002, India

^b Department of Physics, Panjab University, Chandigarh, 160014, India

^c Department of Physics, S. P. University, Vallabh Vidyanagar, 388120, India

Version of record first published: 01 Feb 2007

To cite this article: N. L. Singh, Nilam Shah, C. F. Desai, K. P. Singh & S. K. Arora (2004): Modification of polyethylene terephthalate by proton irradiation, *Radiation Effects and Defects in Solids: Incorporating Plasma Science and Plasma Technology*, 159:8-9, 475-482

To link to this article: <http://dx.doi.org/10.1080/10420150412331296844>

PLEASE SCROLL DOWN FOR ARTICLE

Full terms and conditions of use: <http://www.tandfonline.com/page/terms-and-conditions>

This article may be used for research, teaching, and private study purposes. Any substantial or systematic reproduction, redistribution, reselling, loan, sub-licensing, systematic supply, or distribution in any form to anyone is expressly forbidden.

The publisher does not give any warranty express or implied or make any representation that the contents will be complete or accurate or up to date. The accuracy of any instructions, formulae, and drug doses should be independently verified with primary sources. The publisher shall not be liable for any loss, actions, claims, proceedings,

demand, or costs or damages whatsoever or howsoever caused arising directly or indirectly in connection with or arising out of the use of this material.

MODIFICATION OF POLYETHYLENE TEREPHTHALATE BY PROTON IRRADIATION

N. L. SINGH^{a,*}, NILAM SHAH^a, C. F. DESAI^a, K. P. SINGH^b and S. K. ARORA^c

^aDepartment of Physics, M. S. University of Baroda, Vadodara–390002, India; ^bDepartment of Physics, Panjab University, Chandigarh–160014, India; ^cDepartment of Physics, S. P. University, Vallabh Vidyanagar–388120, India

(Received 10 May 2004; In final form 8 June 2004)

Polyethylene terephthalate (PET) films were irradiated with 3 MeV proton beams at different fluences. The microhardness, electrical, thermal and structural studies were carried out using microhardness tester, LCR meter, thermogravimetric analysis (TGA) and FTIR spectroscopy. Vickers' hardness has been observed to increase with the fluence. The true bulk hardness of the film was obtained at loads greater than 400 mN. The AC electrical conductivity is practically unaffected by irradiation up to a frequency of 10 kHz, but it is found to increase exponentially at a frequency of 300 kHz. The loss factor and dielectric constant are observed to change appreciably with the fluence. It is observed that there is no significant change in the stability of the polymer up to the fluence of 10^{14} ions cm^{-2} as revealed by TGA and FTIR spectroscopy.

Keywords: Polyethylene terephthalate; FTIR; Hardness; Electrical conductivity; Thermal degradation

1 INTRODUCTION

Application of radiation in polymer technology is of great importance in achieving some desired improvement in polymer properties. Ion beam treatment provides a unique way to modify the chemical, structural, optical, mechanical and electrical properties of polymers by causing irreversible changes in their macromolecular structure. It can be used to change, in a controlled way, the physical properties of thin films or to modify the near-surface characteristics of a bulk polymer [1]. The ion beam irradiation affects the polymer structure by cross-linking as well as by degradation [2]. Polyethylene terephthalate (PET) is a soft, transparent thermoplastic with a high melting point ($\sim 265^\circ\text{C}$) and a very good mechanical strength (at least up to 175°C) due to the presence of the aromatic ring in the polymeric structure. It is resistant to heat and moisture and virtually immune to many chemicals and has wide applications. There have been numerous reports on radiation-induced modifications in PET. Steckenreiter *et al.* [3], Biswas *et al.* [4] and Tripathy *et al.* [5] have studied the effects of irradiation by various energetic ions on the physical properties of PET. Bridwell *et al.* [6] have studied the electrical conductivity of PET implanted with 50 keV He^+ , Be^+ , C^+ , N^+ and Ar^+ ions. Changes in surface resistivity and molecular structure induced by 1.6 MeV

* Corresponding author. E-mail: singhnl_msu@yahoo.com

heavy ion irradiation were studied by Ueno *et al.* [7]. Irradiation effects by a 50 MeV Li^{3+} ion beam in PET were studied with respect to their structural and electrical properties by Singh *et al.* [8]. On the other hand, among the mechanical properties, microhardness testing provides a wealth of information regarding deformation processes occurring in semi-crystalline, amorphous, polymeric blends, copolymers and composites. Variation of polymer microhardness has been correlated to differences in crystallinity, molecular weight, cohesive energy density, microstructure, elastic modulus and yield stress [9–12]. It is reported that the differences in processing also affect the resistance of the film to scratching wear. The wear resistance of the films was correlated with the ratio of the hardness to the modulus [12]. However, not much detailed study of change in microhardness, electrical and thermal properties due to ion irradiation has been reported. In this article, the authors report the effects of 3 MeV proton irradiation on the electrical, mechanical and thermal properties of PET at different fluences. The changes in these properties of polymer have been correlated with structural modifications as were observed with the FTIR spectroscopy.

2 EXPERIMENTAL DETAILS

Three pieces of PET ($(\text{C}_{10}\text{H}_8\text{O}_4)_n$; density 1.4 g cm^{-3}) each of thickness $230 \mu\text{m}$ and of size $1.5 \times 1.5 \text{ cm}^2$ were cut from commercially available sheets. These samples were irradiated with 3 MeV protons at the Physics Department, Chandigarh. The beam current density was of the order of 35 nA cm^{-2} and irradiated at three different fluences of 10^{13} , 10^{14} and $10^{15} \text{ ions cm}^{-2}$. The proton beam was made incident perpendicular to the target of diameter 6 mm. All irradiations were performed in vacuum (10^{-6} Torr) at room temperature. To study the structural changes including the alteration in position and intensity of the characteristic bands, the FTIR spectra of all samples were recorded in the wave number range $4000\text{--}500 \text{ cm}^{-1}$ (Bomem Canada, Model-104) with a resolution of 4 cm^{-1} . For microhardness tests, the indenter employed was the Vickers' pyramidal diamond indenter supplied with the microhardness testing accessory of a Carl Zeiss Optical microscope. The electrical properties of all samples were studied after irradiation. The resistance, dielectric loss ($\tan \delta$) and capacitance measurements were carried out using a Hewlett Packard 4284A LCR meter over the frequency range $100 \text{ Hz--}1 \text{ MHz}$ at room temperature. The AC conductivity was calculated using the relation $\sigma = (2\pi f C_p D t) A^{-1} (\Omega^{-1} \text{ cm}^{-1})$. The dielectric constant was calculated using the relation $\varepsilon = C_p / C_0$, where C_p is capacitance measured using the LCR meter and $C_0 = \varepsilon_0 A / t$, where ε_0 is the permittivity of vacuum and A and t are the cross-sectional area and thickness of the sample, respectively. The thermogravimetric analysis (TGA) was recorded using the SIEKO thermal analysis (TGA-220) system in the presence of air from room temperature to 550°C at a predetermined heating rate of $10^\circ\text{C min}^{-1}$.

3 RESULTS AND DISCUSSION

The projected range of 3 MeV proton beam in PET was calculated to be $112 \mu\text{m}$ using SRIM-2000 code [13]. The thickness of the sample is two times more than the projected range. The electronic stopping power $(dE/dx)_e$ and nuclear stopping power $(dE/dx)_n$ were found to be $1.3 \times 10^{-1} \text{ eV \AA}^{-1}$ and 6.58 eV \AA^{-1} , respectively. It was found that 99.94% of the energy is lost due to the electronic interaction.

3.1 FTIR Analysis

The FTIR spectra of the pristine and irradiated samples are shown in Figure 1. The absorption bands as obtained from the pristine spectrum are identified as:

- (a) 725 cm^{-1} : ring deformation of phenyl ring, bending vibration of CH_2 group;
- (b) 862 cm^{-1} : C–H deformation of phenyl ring, vibration band of para substituted benzene ring;
- (c) 1730 cm^{-1} : C=O stretching vibration;
- (d) 2335 cm^{-1} : vibration of CO_2 ;
- (e) 2975 cm^{-1} : C–H stretching of CH_2 group;
- (f) 3068 cm^{-1} : C–H stretching aromatic group;
- (g) 3294 cm^{-1} : C–H stretching vibrations of the alkyne group.

Steckenreiter *et al.* [3] also reported a band at 3294 cm^{-1} assigned to the characteristic C–H stretching mode of the alkyne end group ($\text{R}-\text{C}\equiv\text{C}-\text{H}$). The formation of the alkyne groups is also confirmed by the simultaneous observation of the $\text{C}\equiv\text{C}$ stretching vibration band at 2102 cm^{-1} . The bands in the wave number region from $3600\text{--}2500\text{ cm}^{-1}$ are due to the O–H stretching vibration. The band at 1504 cm^{-1} , corresponds to amorphization of the crystalline fraction and main chain scission at the para position of disubstituted benzene rings [4]. It is observed that there is no change in the overall structure of the polymer but a minor change in intensities has been observed up to the fluence of $10^{14}\text{ ions cm}^{-2}$. This might be due to the breakage of a few bonds in the structure as well as formation of new structures. It may be concluded that PET is resistant to radiation at least up to the fluence of $10^{14}\text{ ions cm}^{-2}$. The spectrum corresponding to the fluence of $10^{15}\text{ ions cm}^{-2}$ indicates a very significant change in the structure of polymer.

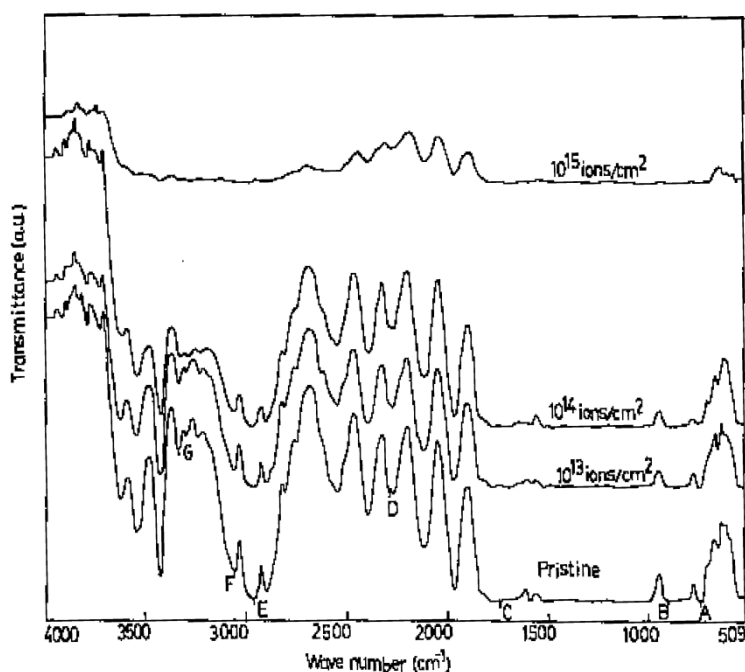


FIGURE 1 FTIR spectra of the pristine and irradiated samples.

3.2 Vickers' Microhardness

For microhardness tests, the indenter employed was Vickers' pyramidal diamond indenter supplied with the microhardness testing accessory of a Carl Zeiss Optical microscope. The microhardness indentations were carried out on the surface of the pristine and irradiated films at room temperature under different applied loads from 100–1000 mN and at a constant loading time of 30 s. The Vickers' diamond pyramidal hardness H_v is the quotient of the applied load P and the pyramidal surface area d^2 of the impression and is given by

$$H_v = \frac{189096 \times P}{d^2}.$$

Figure 2 shows the plot of Vickers' microhardness (H_v) versus applied load (P) as obtained for the pristine and irradiated samples. It is evident from the figure that the microhardness is maximum at the fluence of 10^{14} ions cm^{-2} . The increase in the hardness may be attributed to the cross-linking effect [14, 15]. The hardness is known to be influenced by surface effects. Particularly at low penetration depths, the strain hardening modifies the true hardness of the material. At the higher loads beyond 400 mN, the interior of the bulk specimen is devoid of surface effects. Hence, the hardness value at higher loads represents the true value of the bulk and it is consequently independent of the load. The hardness is seen to increase as fluence increases up to the irradiation fluence of 10^{14} ions cm^{-2} . This may be attributed to the cross-linking phenomenon [14]. However, with increasing fluence, the polymer degrades its mechanical strength and as a result the hardness decreases at the fluence of 10^{15} ions cm^{-2} . The degradation may be a result of scissioning of the chemical bonds at the higher radiation fluences. It is also observed from the FTIR spectra that the structure of the polymer changed at the fluence of 10^{15} ions cm^{-2} .

3.3 AC Electrical Frequency Response

Figure 3 shows the variation of electrical conductivity with log of frequency for the pristine and irradiated samples. A sharp increase in conductivity has been observed around 300 kHz for pristine and irradiated samples. It is also observed that conductivity increases as fluences increase. The increase in conductivity due to irradiation may be attributed to scissioning of polymer chains and as a result to an increase of free radicals, unsaturation, etc. An AC field

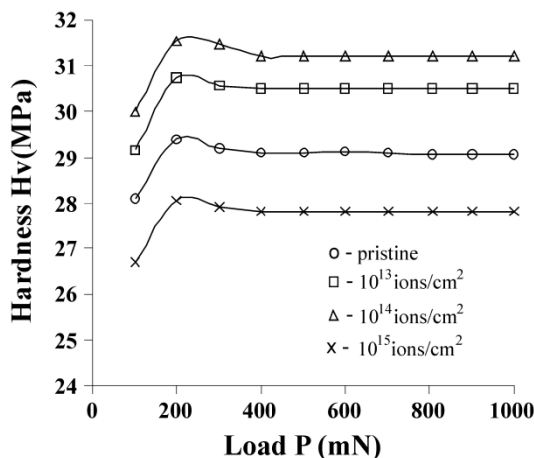


FIGURE 2 The plots of Vickers' hardness versus applied load for pristine and irradiated samples.

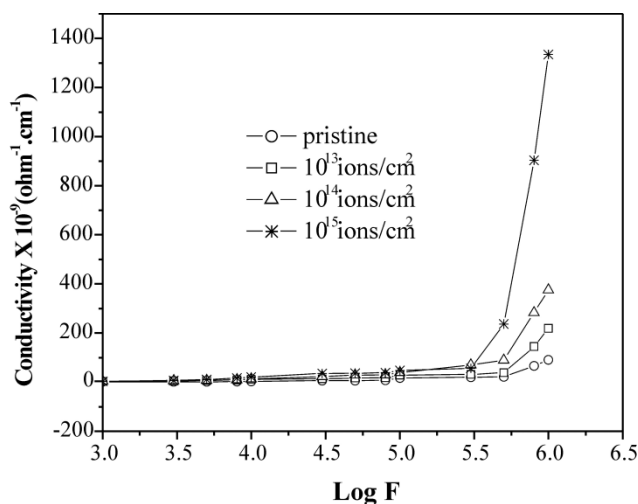


FIGURE 3 AC electrical conductivity versus log frequency at different fluences.

of sufficiently high frequency applied to a metal–polymer–metal structure may cause a net polarization, which is out of phase with the field. This results in AC conductivity, it appears at frequencies greater than that at which traps are filled or emptied [16].

Figure 4 shows the variation of the dielectric constant with frequency for the pristine and irradiated samples. As evident from the plot, the dielectric constant remains almost constant, except when it decreases at sufficiently high frequency where only electronic polarization dominates. At low frequencies, the motion of the free charge carriers is constant and so the dielectric constant remains unchanged. As the frequency increases, the charge carriers migrating through the dielectric get trapped at defect sites and induce an opposite charge in their vicinity, as a result of which they slow down and the value of the dielectric constant decreases.

Figure 5 shows a plot of $\tan \delta$ versus log of frequency for pristine and irradiated samples in the frequency range 300 Hz–1 MHz. It is observed that the variation of $\tan \delta$ with log frequency is identical for pristine and irradiated samples at low frequencies, and higher for irradiated samples at higher frequencies. This possibly indicates the dominance of inductive behaviour. The $\tan \delta$ decreases as frequency increases and becomes negative beyond a frequency of

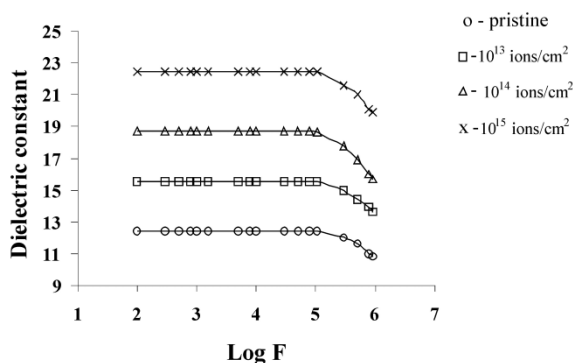


FIGURE 4 The plots of dielectric constant versus log frequency at different fluences.

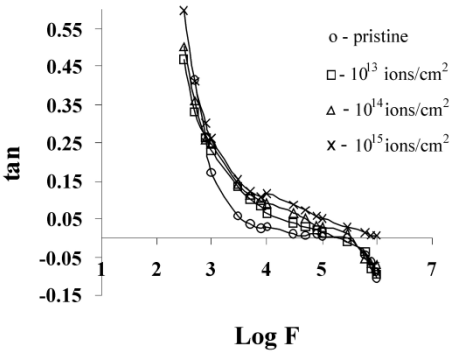


FIGURE 5 The $\tan \delta$ versus log frequency at different fluences.

300 kHz for pristine and irradiated samples up to the fluence of 10^{14} ions cm⁻². This shows the dominance of capacitive contributions [17].

3.4 TGA Analysis

The TGA thermograms of pristine and irradiated samples are shown in Figure 6 and the weight loss (%) at different temperatures for different zones is listed in Table I.

As depicted in Figure 6, the stable zones for pristine and irradiated (at the fluence of 10^{14} ions cm⁻²) samples are the same (up to the temperature of 222 °C) though at the fluence of 10^{15} ions cm⁻², the stable zone is present only up to 127 °C. This change clearly indicates that up to the fluence of 10^{14} ions cm⁻², the system remains reasonably organized but gets quite disorganized with some residual energy when a fluence of 10^{15} ions cm⁻² is used. Some bond formation, *i.e.* forming a more organized structure seems to occur up to the fluence of 10^{14} ions cm⁻². The weight loss of 0.8%, 1.5% and 4.6% has been observed for the

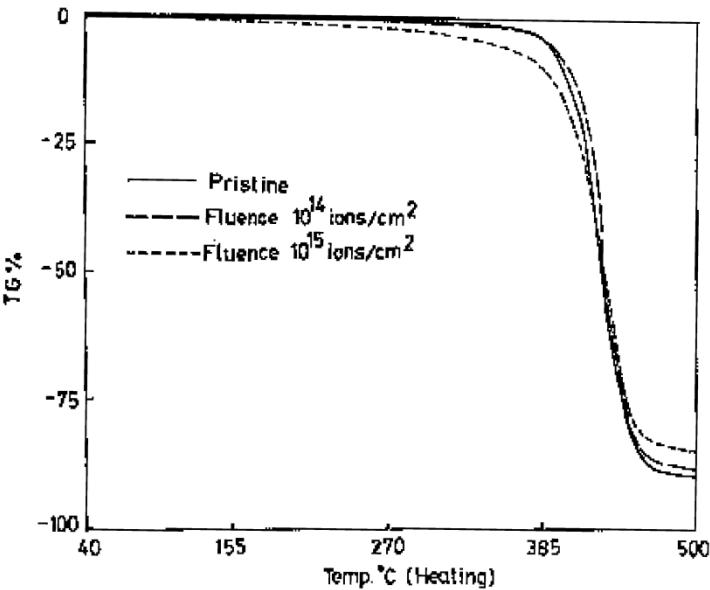


FIGURE 6 TGA thermograms of the pristine and irradiated PET.

TABLE I Weight loss (%) with the temperature for different zones.

<i>Dose</i>	<i>Zone</i>	<i>Temp (°C)</i>	<i>Weight Loss (%)</i>	<i>Interpretation</i>
Pristine	I	40–222	0	Stable zone
	II	222–385	0–3.82	Slow decomposition
	III	385–465	3.82–86.28	Fast decomposition
10^{14} ions cm^{-2}	I	40–222	0	Stable zone
	II	222–385	0–3.82	Slow decomposition
	III	385–465	3.82–84.63	Fast decomposition
10^{15} ions cm^{-2}	I	40–127	0	Stable zone
	II	127–385	0–10	Slow decomposition
	III	385–465	10–81.6	Fast decomposition

pristine and irradiated samples at 10^{14} and 10^{15} ions cm^{-2} , respectively, at the temperature of 343 °C. However, at the temperature of 383 °C, the weight loss of 3.9% has been observed for pristine and irradiated samples (at the fluence of 10^{14} ions cm^{-2}), whereas at the fluence of 10^{15} ions cm^{-2} a weight loss of 10% is observed. From the data, it is evident that no significant change has been observed up to the fluence of 10^{14} ions cm^{-2} , the same fact being also revealed by FTIR spectroscopy (Fig. 1).

4 CONCLUSION

The FTIR spectra indicate that PET gets chemically degraded at the highest proton fluence used, that is 10^{15} ions cm^{-2} . The Vickers hardness of the polymer increases up to a fluence of 10^{14} ions cm^{-2} , probably due to cross-linking without any degradation effect. However, the hardness decreases at the fluence of 10^{15} ions cm^{-2} because of degradation of the polymer due to scissioning of bonds; which is also corroborated by the FTIR spectra. There is an exponential increase in conductivity with log of frequency and the effect is significant at higher fluences. The loss factor ($\tan \delta$) and dielectric constant are observed to change appreciably with the fluences.

Acknowledgements

The authors are thankful to the operating staff of Cyclotron, Department of Physics, Panjab University, Chandigarh and to The Head, Department of Physics, S. P. University, Vallabh Vidyanagar for providing their laboratory facilities and ABS Bayer, Moxi for providing thermal analysis facilities. Financial support given by NSC, New Delhi is gratefully acknowledged.

References

- [1] Mazzoldi, P. and Arnold, G. W. (Eds.) (1987). *Ion beam modification of insulators*, Vol. 2, Chapter 8, Elsevier, Amsterdam, pp. 301–379.
- [2] Lee, E. H. (1999). *Nucl. Inst. Meth.*, **B151**, 29.
- [3] Steckenreiter, T., Balanzat, E., Fuess, H. and Trautmann, C. (1997). *Nucl. Inst. Meth.*, **B131**, 159.
- [4] Biswas, A., Lotha, S., Fink, D., Singh, J. P., Avasthi, D. K., Yadava, B. K., Bose, S. K., Khathing, D. T. and Avasthi, A. M. (1999). *Nucl. Inst. Meth.*, **B159**, 40.
- [5] Tripathi, S. P., Mishra, R., Dwivedi, K. K., Khathing, D. K., Ghosh, S., Fink, D. (2002). *Rad. Eff. Defects Sol.*, **157**, 387.
- [6] Bridewell, L. B., Giedd, R. E., Wang, Y. Q., Mohite, S. S., Jahnke, T., Brown, I. M., Bedell, C. J. and Sofield, C. J. (1991). *Nucl. Inst. Meth.*, **B56/57**, 656.
- [7] Ueno, K., Yasuyo, M., Nobuyuki, N., Mitusuru, N. and Mamoru, S. (1991). *Nucl. Inst. Meth.*, **B59/60**, 1263.

- [8] Singh, N., Sharma, A. and Avasthi, D. K. (2003). *Nucl. Inst. Meth.*, **B206**, 1120.
- [9] Flores, A. and Balta, C. F. J. (1998). *Phil. Mag.*, **A78**, 1283.
- [10] Briscoe, B. J., Sebastian, K. S. and Sinha, S. K. (1996). *Phil. Mag.*, **A74**, 1159.
- [11] Balta, C. F. J. (1985). *Adv. Polym. Sci.*, **66**, 117.
- [12] Beake, B. D. and Leggett, G. J. (2002). *Polymer*, **43**, 319.
- [13] Ziegler, J. F. (2000). SRIM-2000, *The stopping range of ions in matter*, New York, USA: IBM Research, pp. 1–28.
- [14] Lee, E. H., Rao, G. R. and Mansur, L. K. (1997). *Mater. Sci. Forum*, **248/249**, 135.
- [15] Shah, N., Singh, N. L., Desai, C. F. and Singh, K. P. (2003). *Radiat. Meas.*, **36**, 699.
- [16] Jonscher, A. K. (1977). Review Article, The universal dielectric response, *Nature*, **267**, 673.
- [17] Srivastava, A. K. and Virk, H. S. (2000). *Bull. Mater. Sci.*, **23**, 533.